# Investigation of turbulence by microwave imaging reflectometry in the TPE-RX reversed field pinch

Zhongbing SHI, Yoshio NAGAYAMA[1)], Soichiro YAMAGUCHI[2)], Tomokazu YOSHINAGA[1)], Daisuke KUWAHARA[3)], Yoichi HIRANO[4)], Haruhisa KOGUCHI[4)], Satoru KIYAMA[4)], Hajime SAKAKITA[4)] and Kiyoyuki YAMBE[4)]

*The Graduate University for Advanced Studies, Toki 509-5292, Japan*
*Southwestern Institute of Physics, Chengdu, 610041, China*
[1)] *National Institute for Fusion Science, Toki 509-5292, Japan*
[2)] *Kansai University, Suita 564-8680, Japan*
[3)] *Department of Energy Science, Tokyo Institute of Technology, Tokyo 152-8550, Japan*
[4)] *Advanced Industrial Science and Technology, Tsukuba 305-8568, Japan*

(Received: 20 November 2009 / Accepted: 2 February 2010)

The two-dimensional density turbulence around the field reversal surface has been studied by using microwave imaging reflectometry (MIR) in TPE-RX reversed field pinch (RFP). In the standard plasma, the turbulence is intermittent and is dominated by the broad wavenumber spectrum. The turbulence are significantly suppressed when the magnetic relaxation is reduced by using pulsed poloidal current drive (PPCD). In the PPCD plasma, the fluctuation is dominated by the low $n$ mode ($n < 10$). The intermittency is not observed and the PPCD plasma has high confinement as the soft-X-ray (SXR) intensity is significantly increased.

Keywords: turbulence, microwave imaging reflectometry, reversed field pinch

## 1. Introduction

Turbulence is interested by many physicists as it enhances the transport and degrades the overall confinement in the toroidal devices [1]. In the reversed-field pinch (RFP), the plasma has the characteristic of strong fluctuation [1]. The MHD turbulence is known to drive the dynamo, which plays an important role to sustain the plasma configuration in the standard RFP plasmas [2]. The electrostatic turbulence plays an important role in the edge transport [3]. MHD theory suggests that the core RFP dynamo corresponds to the $m = 1$ (low $n$) tearing mode whose resonant surface is located in the inside region [4]. The edge RFP dynamo corresponds to the $m = 0$ tearing mode whose resonant surface is around the field reversal surface. The strong turbulence is expected due to the resonances of $m = 0$ mode, densely packed high $n$ ($m = 1$) modes and high electrostatic turbulence around the reversal surface [1, 3]. Therefore, the fluctuation in the inside region may highly relate to the sustainment of the RFP configuration. So far the edge turbulence of RFP plasma has been reported by electrostatic probes and optical gas-puff imaging ($\rho = 0.96 \sim 1.0$) [5], while the turbulence in the inside region has not been researched due to the inaccessible condition of the probes.

There are two types of operation in the RFP device [6]. The first is the standard RFP formed by steady toroidal induction. Standard plasmas are self-organized via a magnetic relaxation (dynamo) process involving MHD tearing. Previous works showed that the turbulence is also the main cause for energy and particle transport [7]. The second type of plasma is the pulsed poloidal current drive (PPCD) plasma formed by modifying the inductive current drive to reduce the tearing instability [8]. This technique has been demonstrated in several RFP devices. The magnetic turbulence is decreased, and the reduction of the heat and particle transport has been observed in several RFP devices during PPCD [9, 10]. The confinement time has been improved by order of magnitude [8, 10]. Therefore, comparison between the PPCD and without PPCD plasmas is a good example to study the RFP turbulence.

This paper presents the two-dimensional (2D) density fluctuation around the field reversal surface ($\rho \sim 0.8$) in TPE-RX RFP. The turbulence in the standard and the PPCD plasmas are compared. Significant results are as follows: The standard plasma has high turbulence and the fluctuation of microwave imaging reflectometry (MIR) signal is intermittent. The broad spectrum agrees with the multi-helicity (MH) state in the standard plasma. PPCD suppresses the turbulence. The fluctuation in PPCD is dominated by the low $n$ mode, while the high $n$ mode is suppressed.

## 2. Experiments

TPE-RX is a large RFP device with major radius $R$ =1.72 m and minor radius $a$ =0.45 m [11]. It is characterized by a multilayered shell system in a conductive all-metallic vacuum vessel which provides rela-

*author's e-mail: shizb@swip.ac.cn*

tively high $I_p/N$ values ( $10^{-19}$Am; $N = \pi a^2 < n_e >$, the number of electron per unit toroidal length, derived using the line-averaged electron density $< n_e >$). The all-metal first wall also provides MHD mode stabilization and the fast equilibrium control in a short time scale less than millisecond. A six-pulsed PPCD operation has been developed to improve the energy confinement time. The total duration of PPCD is about 18 ms. About ten-fold improvement in confinement has been observed [12]. The operations of the standard and the PPCD plasmas have been reported in Ref. [6].

The plasma density is measured by a double-chord CO2/HeNe laser interferometer in TPE-RX, whose impact parameters, normalized by minor radius $a$, are 0 and 0.69. The density profile is estimated by fitting the experimental data with the following relation [14].

$$n_e(r,t) = n_e(0,t)(1-r^4)(1+C(t)r^4) \qquad (1)$$

where, $n_e(0,t)$ is the core density, $C(t)$ is the profile factor, $r$ is normalized by minor radius $a$. The profile factor $C > 1$ represents the hollow density and $C < 1$ represents the peaked density profile. Both $n_e(0,t)$ and $C(t)$ are determined by the two measured chord values. In TPE-RX, the flat and hollow density profile is often observed in the PPCD and the standard plasmas.

A MIR system has been developed to investigate the turbulence around the reversal surface in TPE-RX. MIR is expected to be a powerful tool to measure the images of the density fluctuation [15, 16]. In the MIR signal $A\exp(i\phi)$, the phase $\phi$ corresponds to the displacement of the cutoff surface in the radial direction. However, the phase $\phi$ is often distorted due to the fringe jumps. The fringe jumps might be removed by numerical algorithm sometimes [13]. The amplitude $A$ corresponds to the reflection power which is scattered by the perpendicular wave on the cutoff surface [17]. The amplitude signal is used to study the turbulence on the cutoff surface in this work.

The detail of the MIR system has been reported in the previous papers [14, 18]. The image of the cutoff surface is made on the detector surface by the optical system. A $4 \times 4$ planar Yagi-Uda antenna array is used. The spatial resolution is 3.7 cm both in toroidal and poloidal directions, so the highest detectable toroidal ($n$) and poloidal ($m$) modenumbers are 292 and 76, respectively. A Gunn oscillator generating the microwave with frequency of 20 GHz is used. The microwave illuminates in the O-mode, so the cutoff density is $n_{ecut} = 0.5 \times 10^{19}$ m$^{-3}$. The experiments with MIR have been performed with the plasma current of 200-300 kA and electron density of $(0.5-1) \times 10^{19}$ cm$^{-3}$. The normalized cutoff radius $r/a$ mainly locates in the region from 0.7 to 0.9 due to the flat or hollow density profile, which is often observed in TPE-RX. This region is near the reversed field surface.

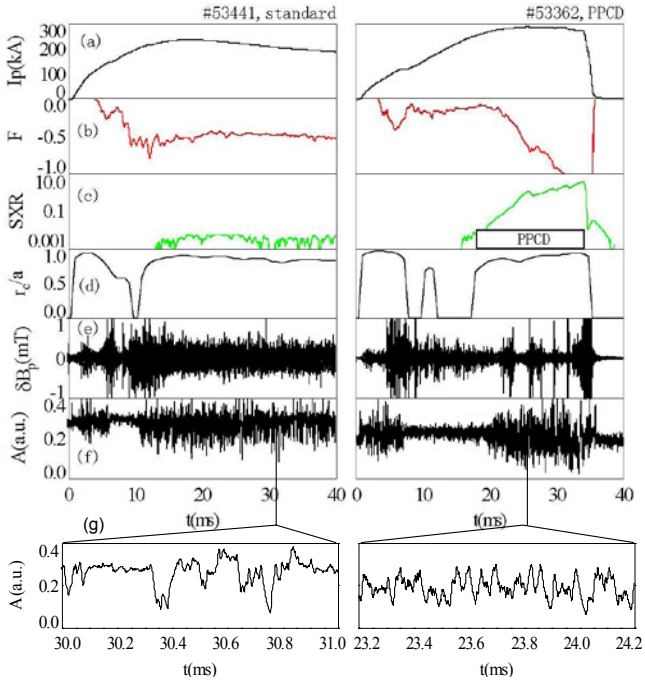


Fig. 1 The plasma parameters, magnetic and MIR signals of the standard ($F = -0.5$) and PPCD plasmas. (a) plasma current $I_p$, (b) reversal parameter $F$, (c) soft-X-ray (SXR) intensity, (d) cutoff radius of MIR,(e) poloidal magnetic fluctuation, (f) and (g) MIR signal.

## 3. Turbulence in standard and PPCD plasmas

Experiments with MIR have been performed in the standard and PPCD plasmas in TPE-RX. In the standard plasma, the reversal parameter $F = B_t(a)/ < B_t >$ is used to identify the strength of the fluctuation as the edge reversal toroidal field $B_t(a)$ is mainly sustained by the turbulence [7]. Here $<>$ denotes average over the whole volume. The deeper $F$ corresponds to the stronger fluctuation in the standard plasma. The magnetic fluctuation becomes more coherent in the deep $F$ plasmas [4]. In the PPCD plasma, the edge toroidal field $B_t(a)$ is mainly driven by the external field, so the $F$ is not an indicative parameter in the PPCD plasmas.

Figure 1 shows the plasma current ($I_p$), the reversal parameter ($F$), soft X-ray (SXR), the normalized cutoff radius ($r_{cut}$), the poloidal magnetic fluctuation and the MIR signal in the standard (# 53441, $F \approx -0.5$) and PPCD (# 53362) plasmas. The rapid increase of the SXR intensity and the rapid decrease of the $F$ are observed after turn on the PPCD ($t \geq 18$ ms). The SXR intensity of the PPCD plasma is about 100 times higher than that in the standard plasma.

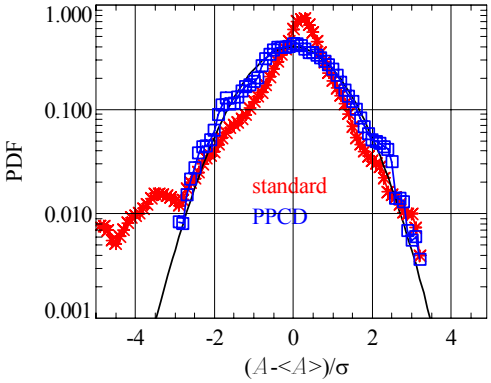


Fig. 2 Probability distribution function of the standard (asterisk, $F = -0.5$) and PPCD (square) plasmas. X-aixs represents the normalized deviation of amplitude of MIR from the average value.

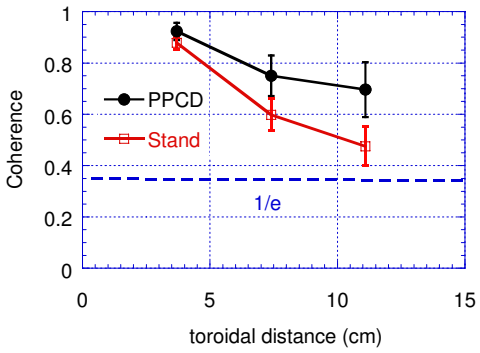


Fig. 3 The toroidal coherence length of the standard (square, $F = -0.5$) and PPCD (dot) plasmas.

This indicates good confinement with PPCD operation. In the standard plasma, $F$ is constant during the flattop of the plasma. Both the standard and the PPCD plasmas have similar cutoff radius $r_{cut} \approx 0.8$ during the flattop of the plasma current. The fluctuation amplitude of MIR signal is very small if there is no cutoff surface in plasma. The standard and the PPCD plasmas have similar fluctuation level. However, their fluctuation structures are different. In the standard plasma, the fluctuation in the amplitude signal is intermittent which bursts mainly in the negative direction. While in the PPCD plasma the fluctuation in the amplitude signal is symmetric.

The poloidal magnetic fluctuation is measured by the complex edge probe (CEP) which is sensitive to the fast magnetic fluctuations [19]. The magnetic fluctuation is suppressed during PPCD, while in the standard plasma ($F = -0.5$, deep $F$) the magnetic fluctuation amplitude is high. It should be noted that the magnetic fluctuation before PPCD is low because of shallow $F$ ($F = -0.15$). Actually, the deep $F$ plasma in the standard RFP has a higher SXR intensity than the shallow $F$ plasma. The SXR intensity of shallow $F$ ($t = 10 - 18$ ms at the right hand side) is much less than that with PPCD. The high magnetic fluctuation at $t = 24 \sim 25$ ms may be caused by the time interval between two PPCD pulses. This can be eliminated by optimization of the operation [20]. After switch off the PPCD operation, the strong magnetic fluctuation is observed at $t = 34 \sim 35$ ms.

Figure 2 shows the probability distribution function (PDF) of the MIR amplitude signals in the standard ($F = -0.5$) and PPCD plasmas. Here, the x-axis represents the normalized amplitude: $(A - < A >)/\sigma$. $< A >$ and $\sigma$ denote the average value and the standard deviation of the amplitude of MIR signal, respectively. The solid line denotes the Gaussian distribution. A non-Gaussian PDF represents the presence of coherent structures or intermittency of ambient turbulence. The PDF of PPCD plasma is similar to the Gaussian distribution, and the fluctuating quantities are limited at the low $(A - < A >)/\sigma$ values (no Gaussian tail). This suggests that the fluctuation in PPCD plasma has been suppressed. In the standard plasma, a strong negative non-Gaussian tail is observed. It corresponds to the negative intermittent bursts of MIR signal (see Fig.1). The non-Gaussian tail is increased as the reversal parameter $F$ is increased in the negative direction. This suggests that the intermittency is increased as the magnetic fluctuation is enhanced in the standard plasma.

The coherence length identifies the size of the fluctuation. The toroidal coherence length is defined as the coherence is decreased to 1/e. Figure 3 shows the toroidal coherence length of the standard (square) and PPCD (dot) plasmas. The coherence is obtained by averaging the toroidal coherence at $f = 10 \sim 100$ kHz. The coherence is decreased as the distance is increased. The coherence length is longer than the detector size. The coherence of PPCD plasma is higher than that of standard plasma. This corresponds to a longer wavelength of the fluctuation in the PPCD plasma. Therefore, the fluctuations in the PPCD plasma have the characteristics of large-scale structures. The fluctuations in the standard plasma have the characteristic of small-scale structures. The toroidal correlation length of the PPCD and standard plasmas at the cutoff surface ($r_{cut} \approx 0.8$) can be estimated from the tendency of the coherence. The estimated correlation length may be larger than 40 cm in the PPCD plasma, while it is about $15 \sim 20$ cm in the standard plasma. The estimated toroidal correlation length at $r_{cut} \approx 0.8$ is similar to the results at $r/a = 1.0$ measured by GPI in TPE-RX [5].

Figure 4 shows the mode spectra of the magnetic fluctuations ($m = 0$ and $m = 1$ modes) as a function of the toroidal modes $n$ in the standard and the PPCD

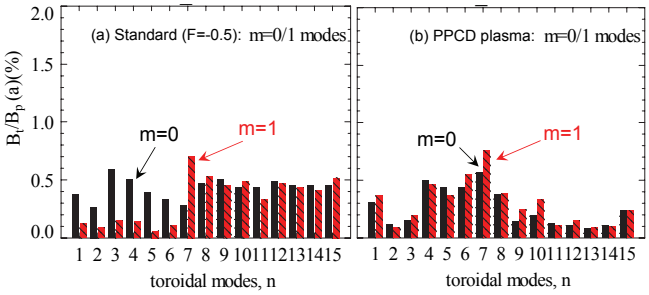


Fig. 4 $m = 0$ and $m = 1$ mode spectra of the standard ($F = -0.5$) and PPCD plasmas. The $n$ and $m$ are the toroidal and poloidal modenumbers, respectively.

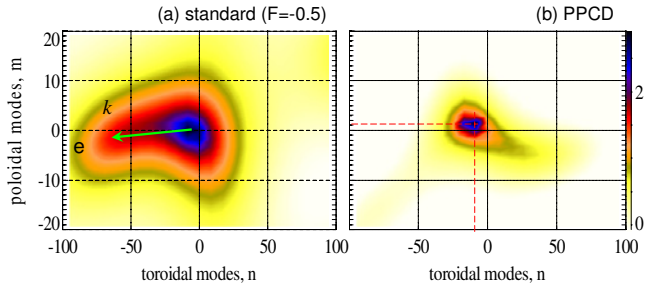


Fig. 5 The 2D mode spectra of the standard ($F = -0.5$) and the PPCD plasmas. The $n$ and $m$ are the toroidal and poloidal modenumbers, respectively.

plasmas. The magnetic fluctuations are obtained by an extensive magnetic measurement system (MMS) [19]. In the PPCD plasma, the amplitude of the $m = 1$ mode is higher than that of the $m = 0$ mode. This may relate to the suppression of the $m = 0$ mode. The fluctuation in the PPCD plasma is dominated by the localized $m = 1$ mode. The low $n$ modes ($n < 10$) have the high fluctuation energy, while the high $n$ modes have very small power. This suggests that the high $n$ modes (or small-scale fluctuations) have been suppressed. The longer coherence shown in Fig. 3 may contribute to the coherence of the low $n$ mode.

In the standard plasma, the power spectra is stronger than that of PPCD plasma. This is as a result of strong magnetic fluctuation. The power of the $m = 0$ modes is higher than the $m = 1$ modes especially for the low $n$ modes. It suggests the global features of the fluctuations ($m = 0$ modes) in the standard plasma. The high $n$ modes are observed in the standard plasma. The wide distribution of $m = 0$ and $m = 1$ modes suggests that the standard plasma is rich of turbulent structures (multi-helicity (MH) state).

Figure 5 shows the 2D modenumber spectra of the standard and the PPCD plasmas by using the MIR amplitude signals. The modenumber spectra are analyzed by the 2D maximum entropy method (MEM) [21, 22]. This method allows us to fit as many peaks to the power spectrum as there are unique values of cross-correlation points. As a result, the location of peak mode becomes clear, especially when the imaged region is smaller than the wave measured. The details of the MEM method have been discussed in [21, 22]. In the PPCD plasma, the fluctuation power is localized in the low $m$ and $n$ ranges, and the spectrum is dominated by a pinpoint ($m = 1\pm1$, $n = -7\pm5$). The mode spectrum of the standard plasma distributes in a wide mode range, especially expands in the toroidal direction. The mode range is ($m = 0 \pm 6$, $n = -70 \sim 20$). The magnetic field is mainly poloidal near $r_{cut} \approx 0.8$. Since the modenumber spectrum has the propagation direction of the modes, the modes mainly propagate in the electron drift direction. The expansion into the high $n$ range suggests presence of many turbulent structures. The analysis of MIR signal is consistent with the multi-helicity state shown in Fig. 4 (a).

## 4. Summary and discussion

In summary, the turbulence around the field reversal surface has been studied by comparing the fluctuations of the standard and the PPCD plasmas. The turbulence in the standard plasma has the features of intermittency. The broad spectrum agrees with the multi-helicity state in the standard plasma. The turbulence are significantly suppressed when the magnetic relaxation is reduced by the PPCD operation. In PPCD, the fluctuation is dominated by the low $n$ mode ($n < 10$), while the high $n$ mode is suppressed. The intermittency is not observed and the confinement is improved.

In this work, the low $n$ mode is measured near the reversal surface by MIR in the PPCD plasma. However, the resonant surface of the low $n$ mode locates in the core region from the MHD theory [1]. Previous measurements showed that the low $n$ mode has the dominant fluctuation amplitude [4]. The measured low $n$ mode near the field reversal surface may be as a result of strong fluctuation in the core region.

The features of the turbulence in the standard and the PPCD plasmas are significantly different. The turbulence and the tearing modes are correlated. This observation supports that suppression of the tearing modes leads to the reduction of the turbulence. Nevertheless, the relation among the turbulence, the tearing modes and magnetic relaxation remains unclear. Further theoretical and experimental works will be needed.

## 5. Acknowledgment

This work is carried out as one of the NINS Imaging Science Project (Grant No. NIFS08KEIN0021). This work is also supported by NIFS (Grant No. NIFS08ULPP525), and SOKENDAI (Grant

No. NIFS08GLPP003). A part of this study was financially supported by the Budget for Nuclear Research of the Ministry of Education, Culture, Sports, Science and Technology of Japan, based on the screening and counseling of the Atomic Energy Commission.

[1] D. Biskamp, *Nonlinear Magnetohydrodynamics* (Cambridge University Press, United Kingdom, 1993) p.289 315.
[2] H.A.B. Bodin Nuclear Fusion **30**, 1717 (1990)
[3] V. Antoni et al., Phys. Rev. lett. **80**, 4185 (1998)
[4] P.R. Brunsell et al., Phys. Fluids B **5**, 885 (1993)
[5] R. Cavazzana et al., Plasma Phys. Control. Fusion **49**, 129 (2007)
[6] H. Koguchi et al., Plasma and Fusion Res. **4**, 022 (2009)
[7] H. Ji et al., Magnetohydrodynamics **38**, 191 (2002).
[8] J. S. Sarff et al., Phys. Plasmas **2**, 2440 (1995)
[9] B. E. Chapman et al., Phys. Rev. Lett. **87**, 205001 (2001).
[10] Y. Yagi et al., Plasma Phys. Control. Fusion **44**, 335 (2002)
[11] Y. Yagi et al., Nucl. Fusion **40**, 1933 (2000)
[12] L. Frassinetti et al., Plasma Phys. Control. Fusion **49**, 199 (2007)
[13] A. Ejiri et al., Plasma Phys. Control. Fusion **39**, 1963 (1997)
[14] Y. Nagayama et al., Plasma and Fusion Res. **3**, 053 (2008)
[15] H. Park et al., Rev. Sci. Instrum. **74**, 4239 (2003).
[16] E. Mazzucato Rev. Sci. Instrum. **69**, 2201 (1998).
[17] Z. Shi et al., J. Plasma and Fusion Res. series **8**, 109 (2009)
[18] S. Yamaguchi et al., Rev. Sci. Instrum. **77**, 10E930 (2006).
[19] K. Yambe et al., Jpn. J. Appl. Phys. **46**, 6831 (2007).
[20] L. Frassinetti et al., Phys. Plasmas **11**, 5229 (2004).
[21] J. Skilling et al., Mon. Not. R. astr. Soc. **211**, 111, (1984)
[22] Z. Shi et al., Plasma and Fusion Res. **4**, S2019 (2009)